Article

Screening and Druggability Analysis of Marine Active Metabolites against SARS-CoV-2: An Integrative Computational Approach

Selvakumar Murugesan[1], Chinnasamy Ragavendran[2], Amir Ali[7,8,9]*, Safir Ullah Khan[9], Velusamy Arumugam[3], Dinesh Kumar Lakshmanan[3], Palanikumar Palanichamy[4], Manigandan Venkatesan[5], Chinnaperumal Kamaraj[6], Zia ur-Rehman Mashwani[8], Muhammad Younas[8], Juan Pedro Luna-Arias[7,9] and Fernández-Luqueño Fabián[7]**

1 Department of Biotechnology, BIT Campus, Anna University, Tiruchirappalli – 620024, Tamil Nadu, India
2 Department of Conservative Dentistry and Endodontics, Saveetha Dental College and Hospitals, Saveetha Institute of Medical and Technical Sciences (SIMATS), Chennai-600 077, Tamil Nadu India
3 Department of Environmental Biotechnology, Bharathidasan University, Tiruchirappalli –620024, Tamil Nadu, India
4 Department of Genomics, School of Biological Sciences, Madurai Kamaraj University, Madurai – 625 021, Tamil Nadu, India.
5 Department of Medicine, University of Texas Health Science Center, Sanantonio, Texas, USA
6 Interdisciplinary Institute of Indian System of Medicine (IIISM), Directorate of Research,SRM Institute Science and Technology, Kattankulathur, Chennai - 603 203.Tamil Nadu, India
7 Nanoscience and nanotechnology program Center for Research and Advanced Studies, National Polytechnic Institute, Mexico City, Mexico
8 Department of Botany, PMAS, Arid Agriculture University, Rawalpindi, Pakistan
9 Department of Cell Biology, Center for Research and Advanced Studies of the National Polytechnic Institute, Av. Instituto Politécnico Nacional 2508, Col. San Pedro Zacatenco, C.P. 07360 Mexico City, Mexico
* Correspondence: ali.amir@cinvestav.mx,and ** venkatesanm@uthscsa.edu

Abstract: The severe acute respiratory syndrome coronavirus 2 (SARS-CoV-2) infections have triggered a recent pandemic of respiratory disease and affected almost every country all over the world. A large amount of natural bioactive compounds is under clinical investigation for various diseases. Especially, marine natural compounds are gaining more attention in the new drug development process. The present study has aimed to identify potential marine-derived inhibitors against the target proteins of COVID-19 using a computational approach. Currently, 16 marine clinical-level compounds were selected for computational screening against the four SARS-CoV-2 main proteases. Computational screening resulted from the best drug candidates for each target based on the binding affinity scores and amino acid interactions. Among these, five marine-derived compounds namely Chrysophaentin A (-6.6 kcal/mol), Geodisterol sulfates (-6.6 kcal/mol), Hymenidin (-6.4 kcal/mol), Plinabulin (-6.4 kcal/mol) and Tetrodotoxin (-6.3 kcal/mol) expressed the minimized binding energy and molecular interactions such as covalent and hydrophobic interactions to the SARS CoV-2 Main Protease. Using Molecular dynamic studies, the Root-Mean-Square Deviation (RMSD), Root-Mean-Square Fluctuation (RMSF), Radius of Gyration (ROG), and Hydrogen bonds (H-Bonds) values were calculated for SARS-CoV-2 Main Protease with Hymenidin docked complex. Additionally, *in silico* Druglikeness and pharmacokinetic property assessments of the compounds demonstrated favorable druggability. These results suggested that marine natural compounds are capable of fighting SARS-CoV-2. Further, *in vitro* and *in vivo* studies need to be carried out to confirm their inhibitory potential.

Keywords: COVID-19; molecular docking; ADMET; marine natural products; Chrysophaentin A; Hymenidin

 doi:10.20944/preprints202212.0008.v1

1. Introduction

COVID-19 is one of the important epidemic diseases caused by Corona virus (SARS-CoV-2) in the current century. It has spread to more than 210 countries and more than, 63 crore people are affected by this disease as on October 2022 (http://www.who.int). In addition, SARS-CoV-2 is a current major challenge for researchers and still they are working on the development of antiviral drugs against SARS-CoV-2 [1,2]. In recent days, Veklury (Remdesivir) and Olumiant (baricitinib) were officially approved by FDA for the treatment of COVID-19 [3–5]. The main symptoms of SARS-CoV-2 include body aches, chest pain, chills with shaking, dry cough, fever, nausea, shortness, and trouble breathing [6]. It primarily affects the respiratory pathway system, infects the lung endothelial cells, and induces inflammatory cell invasion and lymphocytic endothelialitis at the pathological state [7]. SARS-CoV-2 viruses are RNA-based viruses (single-stranded) found in several animal species. The size of the viral genome is nearly 30 kb with a 5′-cap and 3′-poly-A tail. It contains four structural coding genes: Spike, Envelope, Membrane, and Nucleocapsid genes[8,9]. It encodes various structural /non-structural proteins (Nsps), which are produced as cleavage end products of the viral polyproteins (ORF1a and ORF1ab) [10]. 16 Nsps are present in the SARS-CoV-2 viral genome and each has some specific functions such as Nsp1 and Nsp2: suppress the expression of the host gene, Nsp3: formation of multidomain complex, Nsp4, and Nsp6: In transmembrane protein In activity, Nsp5: In protease activity, Nsp7, and Nsp8: primase enzyme, Nsp9: dimerization of RNA, Nsp10: activation of a replicative enzyme, Nsp12: RNA polymerase activity, Nsp13: helicase activity, Nsp14: exoribonuclease activity, Nsp15: endonuclease activity and Nsp16: methyltransferase activity [11,12].

Initially, the viral particles enter the host cell and bind to the enterocytes and pneumocytes. After the replication process, the viral particles are formed and spread into other cells such as cerebral neuronal cells, immune cells, and tubular epithelial cells. The spike protein is used to attach with the host cell protein and it interacts with the angiotensin-converting enzyme-2 (ACE-2) [13]. Once the viral particles enter the host cells, they are released into the genome along with the nucleocapsid. The ORF1a and ORF1ab produced the two polyproteins, pp1a and pp1b which enable the translation process using the ribosome of the host cell. Both the pp1a and pp1b polyproteins help to form a replication /transcription complex[14]. Currently, researchers and scientists are working on the development of a drug against COVID-19 by following the ways such as prevention of self-assembly (structural proteins), viral replications (Nsps), viral entry, and blocking of signaling pathways required for viral infections[15].

The marine environment possesses various spectra of species (i.e. animals and plants such as seaweeds), which contribute to yielding major economic growth across the globe [16]. Marine algae, corals, jellyfish, sharks, seaweeds, and sponges are potentially active renewable resources and they have been used for food, medicine, and nutraceutical prospects around the world[17]. Recently, biomedical researchers are focusing on drug discovery using natural sources especially, the marine natural products (MDPs). Numerous MDPs have been reported as having various pharmacological and biological activities such as antibiotic, anticancer, anti-inflammatory, antiviral, and neuroprotective properties. Cytarabine (Ara-C) is the first marine-derived anticancer agent, isolated from marine sponges and it blocks the DNA polymerase function in the cancer cells. It was approved for the treatment of leukemia by FDA in 1969 [18]. Totally, 18 MDPs are involved in clinical trials (Phase-I: four, Phase-II: eight, Phase-III & IV: six) and four marine-derived compounds (Brentuximab vedotin, Cytarabine, Eribulin mesylate, Trabectedin) have been approved and available in the market. The pharmaceutical pipeline comprising approved and developmental MDPs offers new hopes and new tools in the treatment of COVID-19 patients. The findings of the present study will deliver valuable data for the development of MDP derivatives as lead structures, novel therapeutic and prophylaxis drug candidates against COVID-19 in the near future.

 doi:10.20944/preprints202212.0008.v1

2. Materials and methods

2.1. Software/ servers used

PubMed Database, PubChem Database, RCSB Protein Data Bank, pkCSM – pharmacokinetics online server, DruLiTo 1.0.0 software, Open Babel v2.3, PyRx 0.8, and Discovery studio 2017R2.

2.2. Target protein preparation

The 3D crystal structures of SARS-CoV-2 main protease (6LU7; 2.16 Å), were collected from the Protein Data Bank (https://www.rcsb.org/). The unnecessary molecules such as ions, inhibitors, ligands, heteroatoms, and water molecules were removed from the COVID-19 target protein structure using BIOVIA Discovery Studio. The target protein structures were loaded in PyRx version 0.8 and converted into PDBQT format[19].

2.3. Ligand preparation

The marine active compounds (preclinical and clinical levels) were used for ligand preparation (Table 1). The 3D structures of the selected marine bioactive were collected from the PubChem Database (https://pubchem.ncbi.nlm.nih.gov/) in SDF file format. Initially, the ligand files were loaded and energy was minimized by Open Babel (MMFF94 method). After the energy minimization process, the ligand files were converted into PDBQT format. These energy-minimized ligands were subjected to further docking analysis [20].

Preprints (www.preprints.org) | NOT PEER-REVIEWED | Posted: 1 December 2022 doi:10.20944/preprints202212.0008.v1

Table 1. Physiochemical properties of marine derived clinical level compounds using DruLiTo software.

Compound	MW	log P	Alog P	HBA	HBD	TSPA	AMR	nRB	nAtom	RC	n RigidB	nArom Ring	nHB
Cytarabine, ara-C	243.09	-2.193	-2.942	8	4	128.61	52.82	2	30	2	16	0	12
Vidarabine, ara-A	267.1	-2.367	-3.453	9	4	136.26	62.91	2	32	3	19	2	13
Tetrodotoxin	319.1	-3.581	-4.239	11	8	190.25	61.71	1	39	4	24	0	19
DMXBA	308.15	1.262	-0.538	4	0	43.18	97.19	4	43	3	21	2	4
Plinabulin	336.16	3.008	0.565	6	3	82.59	102.06	3	45	3	24	2	9
Pseudopterosin A	432.25	4.368	0.885	6	4	99.38	119.61	3	67	4	31	1	10
Chrysophaentin A	676.02	5.424	3.052	8	6	139.84	187.65	0	68	5	48	4	14
Phenethylamine	121.09	1.106	0.725	1	1	26.02	43.12	2	20	1	7	1	2
Geodisterol sulfates	506.27	5.203	1.597	6	3	112.44	139.82	7	77	4	31	1	9
Bromophycolides	662.02	6.273	4.125	4	2	66.76	145.79	1	71	3	35	1	6
Plakortin	312.23	5.484	0.253	4	0	44.76	80.06	9	54	1	13	0	4
Homogentisic acid	168.04	0.036	-0.123	4	3	77.76	44.72	2	20	1	10	1	7
Hymenidin	309.02	0.93	-1.68	6	4	91.54	72.63	5	30	2	14	2	10
Dysidine	451.2	6.237	0.807	7	3	129.15	120.8	6	64	3	27	0	10
Capnellene	220.18	3.585	1.41	1	1	20.23	65.87	0	40	3	18	0	2
Pulicatin A	223.07	0.881	0.66	3	2	78.12	65.21	2	28	2	14	1	5

MM: molecular mass, HBD: hydrogen bond donors, HBA hydrogen bond acceptors, PSA: polar surface area, AMR: Atom Molar Refractivity, nRB: number of Rotatable Bond (MM less than 500 Da, no more than 5 HBD, no more than 10 HBA, and partition coefficient (log P) not greater than 5, TPSA no greater than140 Å2, AMR: 40 to 130, nRB: not more than 3 RB).

2.4. Druglikeness calculations

The Druglikeness analysis was performed to analyze the structural and physicochemical properties of potent hits such as atom molar refractivity (AMR), octanol-water partition coefficient (AlogP), H-bond acceptor (HBA), H-bond donor (HBD), partition coefficient (logP), molecular weight (MW), number of rotatable bonds (nRB), number of Atom, total polar surface area (TPSA), etc., using DruLiTo software. The different molecular property filters such as CMC-50-like rule [AlogP (1.3 – 4.1); Molecular refractivity (70 – 110); Molecular weight (230 – 390); Number of Atoms (30 – 55)], BBB likeness [No. of hydrogen bonds (8-10); Molecular weight (400 -500); No acids], Ghose filter [logP (-0.4 – 5.6); Molar refractivity (40 – 130); Molecular weight (160 – 480); Number of Atoms (20 – 70); Polar surface area < 140], MDDR-like rule [No. of Rings ≥ 3; No. of Rigid bonds ≥ 18; No. of Rotatable bonds ≥ 6], QED rule [Molecular weight; AlogP No. of Hydrogen-bond acceptors; No. of Hydrogen-bond donors; No. of Rotatable bonds; Polar surface area No. of Aromatic bond count; No. of Structural alerts] and Veber rule [No. of Rotatable bonds ≤ 10; Polar surface area ≤ 140] were applied [21].

2.5. Prediction of pharmacokinetic parameters

In silico ADMET (Absorption, Distribution, Metabolism, Excretion, and Toxicity) analysis was performed to analyze the pharmacokinetic properties of the potent hits, such as absorption (water solubility, intestinal absorption, Caco-2 and skin permeability) distribution (blood-brain barrier (BBB), Central Nervous System (CNS) permeability, volume of distribution at steady-state (VDss)), metabolism, excretion (drug clearance) and toxicity

 doi:10.20944/preprints202212.0008.v1

(LD50, AMES, chronic acute, and hepatotoxicity) by using the pkCSM online server (https://biosig.lab.uq.edu.au/pkcsm/) [22].

2.6. Molecular docking studies

Following ligand and protein preparation, molecular docking was performed based on the grid box approach (X = − 26.28, Y = 12.60, Z = 58.97) using AutoDock Vina inbuild PyRx version 0.8 (Dallakyan & Olson, 2015). The docking analysis of COVID-19 proteins with bioactive drug candidates was evaluated by the binding affinities (kcal/mol). After docking analysis, the docked complex files were subjected to interaction studies. The protein and the ligand complex were loaded in the BIOVIA Discovery studio and different types of interactions such as covalent, carbon-hydrogen (C-H), hydrophobic interactions and Van der Waals attractions were analyzed [23].

2.7. Molecular dynamic stimulation

MD simulation for the target SARS-CoV-2 Main protease and Hymenidin was carried out in GROMACS 2020.4 using Amber ff19SB force field [24,25] and WebGRO online server (https://simlab.uams.edu/index.php). The lowest binding energy (most negative) docking conformation generated by AutoDock was taken as the initial conformation for MD simulation. The target protein topology parameter was generated using GROMACS but the topology for Hymenidin was created using acpype [26–28]. After creating the topology complex, the complex was submerged in a dodecahedron box of simple point charge (SPC) water molecules. Next, the complex was energy minimized by steepest descents for 50000 steps. The next step is to equilibrate the complex, for this, the solute is exposed to position-restrained dynamics simulation at 300k and also at 300ps. The final step is the MD production run and the run is subjected to 300K temperature and pressure at 1bar for 10ns.

MD simulation of SARS-CoV-2 Main protease and Hymenidin complex was performed by online WebGRO server for 50ns. Initially, the Hymenidin topology file was prepared using PRODRG server (http://davapc1.bioch.dundee.ac.uk/cgi-bin/prodrg). The GROMOS96 43a1 force field was used for this study and the SARS-CoV-2 Main protease and Hymenidin files energy minimized by steepest descents for 50000 steps. The calibration of NVT/ NPT was completed at 300 K and 1 bar pressure. From the MD stimulation, the Root-Mean-Square Deviation (RMSD), Root-Mean-Square Fluctuation (RMSF), Radius of Gyration (ROG), Hydrogen bonds (H-Bonds) values were examined for SARS-CoV-2 Main protease and Hymenidin docked complex [29].

3. Results and discussion

MDPs have been used as both nutraceuticals and medicinal agents for the treatment of various health illnesses. Especially, marine secondary metabolites play an important role in pharmacological research. Druglikeness properties are important features for drug design[30]. Moreover, the rapid development of high throughput screening, (computational approaches) to rational drug design and new bioactive molecules from natural sources was an activity of the past. 16 clinical and preclinical bioactive compounds from the marine ecosystem were selected for the present study (Fig. 1). A flowchart of the molecular docking approach is given in Fig. 2.

Preprints (www.preprints.org) | NOT PEER-REVIEWED | Posted: 1 December 2022 doi:10.20944/preprints202212.0008.v1

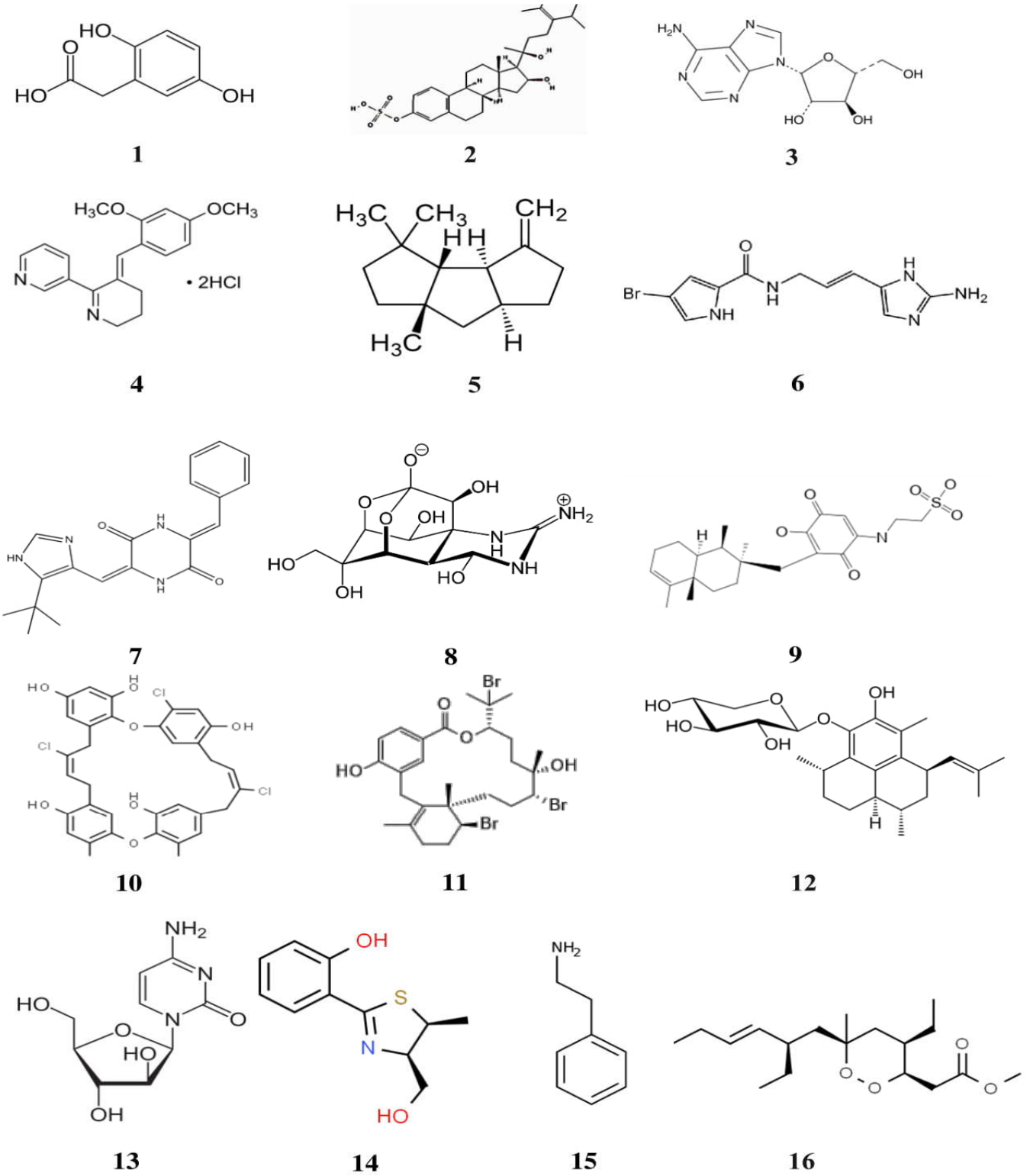

Figure 1. List of marine-derived preclinical and clinical level compounds.

1. Homogentisic acid, 2. Geodisterol sulfates, 3. Vidarabine, ara-A, 4. DMXBA (GTS-21), 5. Capnellene, 6. Hymenidin, 7. Plinabulin, 8. Tetrodotoxin, 9. Dysidine, 10. Chrysophaentin A, 11. Bromophycolide, 12. Pseudopterosin A, 13. Cytarabine, 14. Pulicatin A, 15. Phenethylamine, 16. Plakortin.

Preprints (www.preprints.org) | NOT PEER-REVIEWED | Posted: 1 December 2022 doi:10.20944/preprints202212.0008.v1

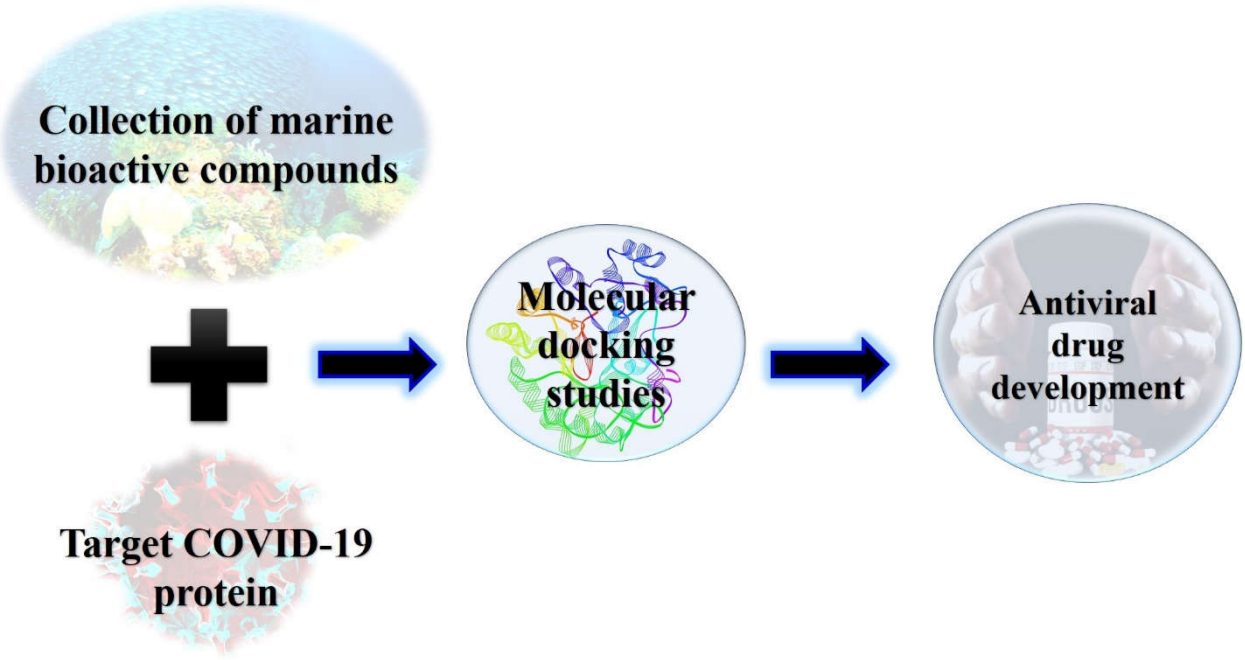

Figure 2. Schematic diagram of the workflow of *in silico* docking study on marine-derived clinical compounds.

3.1. Drug-likeness properties

The physicochemical properties including lipophilicity, hydrogen bonding, and compound molecular weight (MW), are important in the drug development process, indeed it influences the pharmacokinetic properties of the drug compound includes absorption, membrane permeability, distribution, drug clearance, etc. Initially, all the compounds were subjected to drug likeliness analysis. Among these compounds, 11 bioactive compounds (Bromophycolides, Capnellene, Cytarabine, ara-C, DMXBA, Homogentisic acid, Hymenidin, Phenethylamine, Plinabulin, Pseudopterosin A, Pulicatin A, Vidarabine, ara-A) obeyed Lipinski's rule (Table. 1). Similarly, 9 compounds (Pulicatin A, Capnellene, DMXBA, Homogentisic acid, Hymenidin, Plakortin, Plinabulin (NPI-2358), Pseudopterosin A, β-carboline) obeyed Ghose rule and 6 compounds (Pulicatin A, Capnellene, DMXBA, Phenethylamine, Plakortin, β-carboline) followed BBB-Likeness rule. Except for the alkaloids class of Plinabulin, other compounds not followed the CMC-50-like rule. All marine drug compounds obeyed the CMC-50-like rule except Tetrodotoxin. Similarly, Chrysophaentin A and Tetrodotoxin also not followed the QED rule. In addition, expect Dysidine and Geodisterol sulfates remaining all compounds were not obeyed the MDDR-like rule [21]. The physiochemical of the bioactive agents would be an important determinant of their permeability and lipophilicity [31].

3.2. Molecular docking studies

SARS-CoV-2 Main Protease is an important enzyme mainly involved in the replication within the host system. To inhibit this enzyme activity, viral replication should be prevented [32,33]. Because no homolog of SARS-CoV-2 main protease has been identified in humans, it is achievable to develop effective and specific SARS-CoV-2 main protease inhibitors with extremely weak inhibitory activities on human proteases, thereby reducing the side effects caused by SARS-CoV-2 Main Protease inhibitors[32]. It contains three domains: Domain – I (8 – 101), Domain – II (102 – 184), and Domain – III (201 – 303). Domain – I and Domain – II have an anti-parallel β-barrel structure and Domain – III has five α-helices. The substrate-binding site of SARS-CoV-2 main protease is located between Domain – I and Domain – II.

Preprints (www.preprints.org) | NOT PEER-REVIEWED | Posted: 1 December 2022 doi:10.20944/preprints202212.0008.v1

The marine-derived preclinical, clinical, and approved drug candidates were docked with SARS-CoV-2 Main protease, using PyRx version 0.8 and the results were tabulated (Table. 2). The Geodisterol sulfates and Chrysophaentin A were tightly bound to the COVID-19 targets of the Main protease, complex with minimized binding energy (-6.6 kcal/mol). Plinabulin and Hymenidin bioactive docked complex expressed the second highest binding affinity (-6.4 kcal/mol) compared with the other drug molecules. The molecular docking results were compared to the standard Hydroxychloroquine (HCQ), and paracetamol (Table 2).

The marine bioactive compounds were more bound to Domain – I and Domain – II residues rather than Domain – III. The virtual screening using the receptor grid docking at the cleft of domain I and domain II active site. Geodisterol sulfates (Marine steroidal compound) and SARS-CoV-2 Main Protease complex showed the four hydrophobic interactions (Pi-Sigma: VAL104; 3.857Å, Alkyl: VAL104; 4.436Å, VAL104; 4.242Å, Pi-Alkyl: PHE294; 4.412Å) with the Domain – I and Domain – III. The docked complex of Chrysophaentin A and SARS-CoV-2 Main Protease formed the three hydrogen bond interactions (GLU290; 2.576Å, LYS137 2.938Å, LYS5; 3.099Å), two alkyl hydrophobic interactions (LYS137 4.531Å, TYR126 4.243Å) and one electrostatic interaction with the amino acid LYS137 (4.561Å) with all domains (Fig. 3). Hymenidin is an alkaloid class of marine bioactive compound bound to the SARS-CoV-2 Main Protease and that showed highest covalent interactions with a suitable binding affinity (-6.4 kcal/mol). Hymenidin interacted with SARS-CoV-2 protease by forming four hydrogen bond interactions with the amino acids of SER158 (2.466Å), ASP153 (2.359 Å), ASN151 (2.461Å), ASP295 (2.324Å) and two hydrophobic interactions with the amino acid of VAL104 (3.809; Alkyl and 4.539; Pi-Alkyl) with Domain – II and Domain – III (Fig. 3). Plinabulin also an alkaloid class of marine bioactive compound, bound complex exhibited the one H-bond interaction (GLN110; 2.502 Å), one C-H interaction (GLN110; 3.497 Å) and two hydrophobic interactions (Pi-Sigma: THR111; 3.638 Å, Pi-Alkyl: PHE294; 4.464 Å). The alkaloid class of Tetrodotoxin with SARS-CoV-2 Main Protease complex showed one H-bond interaction (ASN151; 2.67 Å), two electrostatic interactions (ASP153; 5.335 Å, PHE 294; 4.993 Å). HCQ is an anti-malarial drug, that has been suggested for the treatment of COVID-19. HCQ with SARS-CoV-2 Main Protease docked complex showed two H-bond interactions (GLN110; 2.608Å, THR111; 2.187Å) and 231 four hydrophobic bonding (ILE106; 3.686Å, VAL101; 5.298Å, VAL104; 4.594Å) with 232 significant binding energy (-6.6 kcal/mol). In addition, the alkaloid class of Plinabulin was also bound to the same binding region of SARS-CoV-2 Main Protease (GLN110, THR111). Paracetamol can help to relieve symptoms associated with COVID-19. The protein-ligand interaction of paracetamol and SARS-CoV-2 Main Protease formed the three hydrogen bond interactions (THR111; 234 2.925Å, ASN151; 3.083Å, ASP295; 2.73Å) to the amino acid residues. Similarly, the alkaloid class of Hymenidin was also bound to the same binding region of SARS-CoV-2 Main Protease (ASN151, ASP295).

7,2''-Bieckol (MW 742.5) is a phlorotannin, mainly found in *Ecklonia cava* (brown algae). The docking results of 7,2''-Bieckol and SARS-CoV-2 Main protease showed the lowest binding energy (-10.78 kcal/mol) compared with standard drugs Lopinavir (-9.23 kcal/mol) and Remdesivir (-9.00 kcal/mol) using MOE 2016.0802. This protein ligand complex showed four H-bond formations (THR24, THR26, GLY143 AND GLU189), and the drug compound is mainly involved in Domain – I and Domain – II [34]. Similarly, Hymenidin docked complex also displayed the four H-bond interactions in Domain – II and Domain – III. Avarol, a sesquiterpenoid hydroquinone found in Dysidea avara (sponge) and mainly used as an antiviral agent. Avarol and SARS-CoV-2 Main protease displayed one H-bond interaction (GLN 189) and seven hydrophobic interactions (HIS41, HIS164, MET49, MET165, CYS44, ASP187, ARG188) in Domain – I and Domain – II. Chrysophaentin A docked complex exhibited the three hydrogen bond interactions (GLU290, LYS137, LYS5), two alkyl hydrophobic interactions (LYS137, TYR126), and one electrostatic interaction with the amino acid (LYS137) with all Domains (I, II and III) [35]. The molecular docking studies for SARS-CoV-2 Main protease and *Clathria Sp.* (marine sponge) natural

Preprints (www.preprints.org) | NOT PEER-REVIEWED | Posted: 1 December 2022 doi:10.20944/preprints202212.0008.v1

compounds (Clathrin-A; -6.67 kcal/mol, Clathrin-B -7.09 kcal/mol, Clathsterol; -2.20 kcal/mol, and Mirabilin-G; -7.38 kcal/mol). Among these four compounds, Clathsterol showed four H-bond formations (CYS145, HIS163, THR26, GLY143) and Mirabilin-G showed one H-bond formation (GLU166) in Domain – I and Domain – II [36]. According to [37] the docking studies for 57 antiviral marine alkaloids with SARS-CoV-2 Main protease. Two marine alkaloids (manzamine A; -10.2 kcal/mol) and 8-hydroxymanzamine; -10.5 kcal/mol) were displayed the minimized binding energy in Domain – II than the standard drugs (darunavir; -7.9 kcal/mol and lopinavir; -7.4 kcal/mol) against SARS-CoV-2 Main protease.

Table 2. The binding energy values of the marine-derived clinical level compounds to the SARS-CoV-2 Main Protease using PyRx version 0.8 0.8 (Unit- kcal/mol).

S. No	Compound name	PubChem ID	Chemical class	Main Protease (6LU7)
1	Homogentisic acid	780	Phenolics	-5.6
2	Phenethylamine	1001	Alkaloid	-4.8
3	Cytarabine, ara-C	6253	Nucleoside	-6.2
4	Vidarabine, ara-A	21704	Nucleoside	-6.1
5	DMXBA (GTS-21)	5310985	Alkaloid	-5.5
6	Hymenidin	6439099	Alkaloid	-6.4
7	Plinabulin	9949641	Alkaloid	-6.4
8	Dysidine	10321583	Terpene	-5.9
9	Tetrodotoxin	11174599	Alkaloid	-6.3
10	Pseudopterosin A	11732783	Glycoside	-6.3
11	Capnellene	14060593	Terpene	-6.0
12	Bromophycolides	21778345	Terpene	-6.0
13	Geodisterol sulfates	44254699	Steroid	-6.6
14	Plakortin	44417613	Polyketide	-5.4
15	Chrysophaentin A	46872004	Shikimate	-6.6
16	Pulicatin A	136020617	Alkaloid	-5.5
17	Paracetamol	1983	Standard drug	−6.2
18	HCQ	3652	Standard drug	-6.6

Table 3. Molecular interactions of the selected marine derived clinical level compounds to the SARS-CoV-2 Main Protease using Discovery Studio 2017R2.

Compound name	Main Protease (6LU7)
Geodisterol sulfates	VAL104, PHE294
Chrysophaentin A	GLU290, LYS137, LYS5, TYR126
Hymenidin	SER158, ASP153, ASN151, ASP295, VAL104
Plinabulin (NPI-2358)	GLN110, THR111, PHE294
Tetrodotoxin	ASN151, ASP153, PHE 294
Paracetamol	THR111, ASN151, ASP295
HCQ	GLN110, THR111, ILE106 , VAL101, VAL104

Preprints (www.preprints.org) | NOT PEER-REVIEWED | Posted: 1 December 2022 doi:10.20944/preprints202212.0008.v1

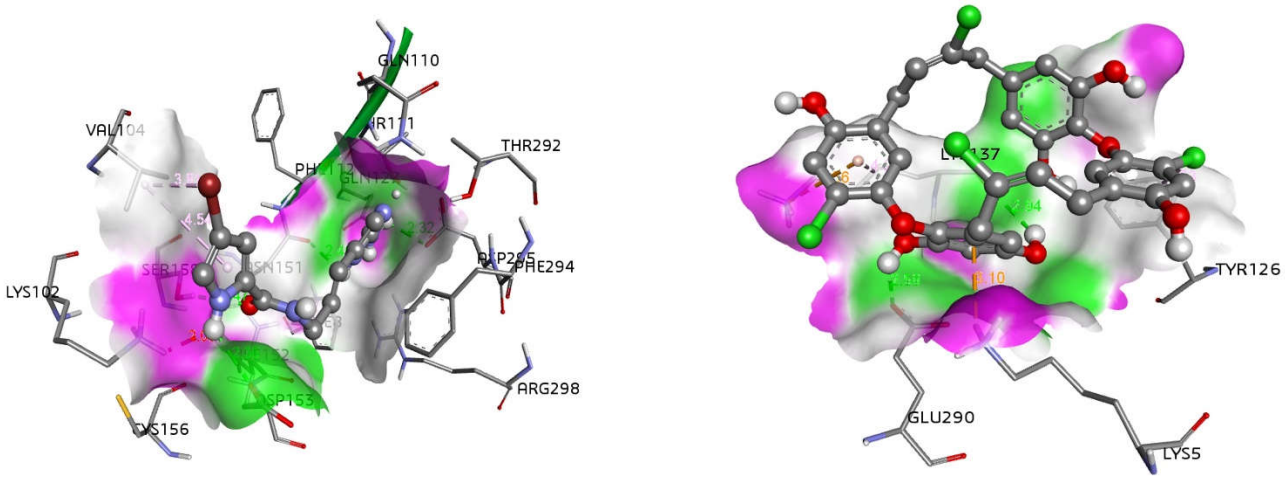

Hymenidin with SARS-CoV-2 Main Protease enzyme

Chrysophaentin A with SARS-CoV-2 Main Protease enzyme

Figure 3. Non-covalent interactions and hydrogen bonding surface map between SARS-CoV-2 Main Protease enzyme and marine clinical level compounds (i. Hymenidin with SARS-CoV-2 Main Protease; ii. Chrysophaentin A with SARS-CoV-2 Main Protease).

3.3. Molecular dynamics stimulation

MD stimulation is a computer-based approach, used to predict the stability of the protein-ligand complexes, conformational flexibilities, and the dependability of protein-ligand affinities. Therefore, a marine active compound of Hymenidin with a low SARS-CoV-2 Main Protease docking score was submitted for MD simulations followed by binding energy calculations.

Temperature and pressure parameters were simulated for 300 ps at 300 K and 1 bar pressure, respectively. The Hymenidin with SARS-CoV-2 Main Protease docked complex showed stability conformation through the MD run for 10ns. Hymenidin with SARS-CoV-2 Main Protease docked complex showed the deviation during the initial stimulations and RMSD value was obtained and the obtained value was below 0.25nm and the average standard deviation is less than 0.11nm which is negligible (Fig. 4). Similar results were found by [38,39]. The considerable variations were noticed within a short period of 2 ns to 4 ns MD run in HCQ with SARS-CoV-2 Main Protease docked complex [38]. In addition, curcumin with SARS-CoV-2 Main Protease docked complex showed 0.08–0.3 with an average of 0.19 nm [39]. Furthermore, Tinosponone with SARS-CoV-2 Main Protease docked complex exhibited the RMSD value below 0.2 nm and the average deviation was around 0.12 nm [40].

The radius of gyration (ROG) is a physical parameter, used to calculate the distance between the center of mass of the protein (SARS-CoV-2 Main Protease) taken with its rotational axis. ROG analysis for the SARS-CoV-2 Main Protease with Hymenidin was examined for 50 ns at 300 K temperature and 1 bar pressure optimized condition. The average value of ROG for Hymenidin with SARS-CoV-2 Main Protease was found around 2.1 to 2.2 nm (Fig. 5). It represents the conformational stability of the formed protein-ligand complex between the SARS-CoV-2 Main Protease and Hymenidin. According to [41] commercial drugs (such as 5-fluorouracil, methotrexate, and paclitaxel) found similar ROG values around 2.0 to 2.2 nm.

Root mean square deviation (RMSD) is used to examine the conformational stability of protein-ligand complex (SARS-CoV-2 Main Protease-Hymenidin) and it is defined as the "square root of an average value of the square of coordinate values of the protein". High values of RMSD values represent the conformational instability of docked complex. In general, RMSD value should be 2 to 3 Å. In the present study, SARS-CoV-2 Main Protease-Hymenidin docked complex showed less than 3 Å RMSD value (0.1 to 0.23 nm) in Fig. 6. This RMSD value indicates that the alkaloid class of Hymenidin was tightly bound

Preprints (www.preprints.org) | NOT PEER-REVIEWED | Posted: 1 December 2022 doi:10.20944/preprints202212.0008.v1

to the SARS-CoV-2 Main Protease and are showed in an acceptable range. According to [33] the cyclic depsipeptide of plitidepsin (from ascidian) with SARS-CoV-2 Main Protease showed similar RMSD values with fluctuation around 0.3 nm at 300 K until 50 ns run.

Root mean square fluctuation (RMSF) is similar to the RMSD and it is an important parameter to define the flexible areas as of a protein-ligand system. It mainly involves individual amino acid residue flexibility. It is used to explore the conformation stability due to the individual amino acids of the SARS-CoV-2 Main Protease in the complex form with Hymenidin. Fewer fluctuation coordinates represent more stability. The RMSF value of SARS-CoV-2 Main Protease-Hymenidin docked complex was calculated to be between 0.1 to 0.5 nm at 300 K temperature and 1 bar pressure optimized condition (Fig. 7). The RMSD and RMSF for the SARS-CoV-2 Main Protease-Hymenidin complex showed that the stable binding throughout 50 ns. The stable RMSD and RMSF showed that the Hymenidin had a strong binding affinity to the SARS-CoV-2 Main Protease and may be reasonable to act as a good inhibitor against SARS-CoV-2 Main Protease. H-bond interaction is important for docking studies. It can be classified into two types: i) conventional and non-conventional H-bonding. Non-conventional H-bonding places a vital role in molecular docking studies [42]. Because the stability of the small molecule in the active binding region of the protein is calculated in terms of an average number of non-conventional H-bonds. In the present study, the docked complex formed a maximum of four H-bond interactions (Fig. 8).

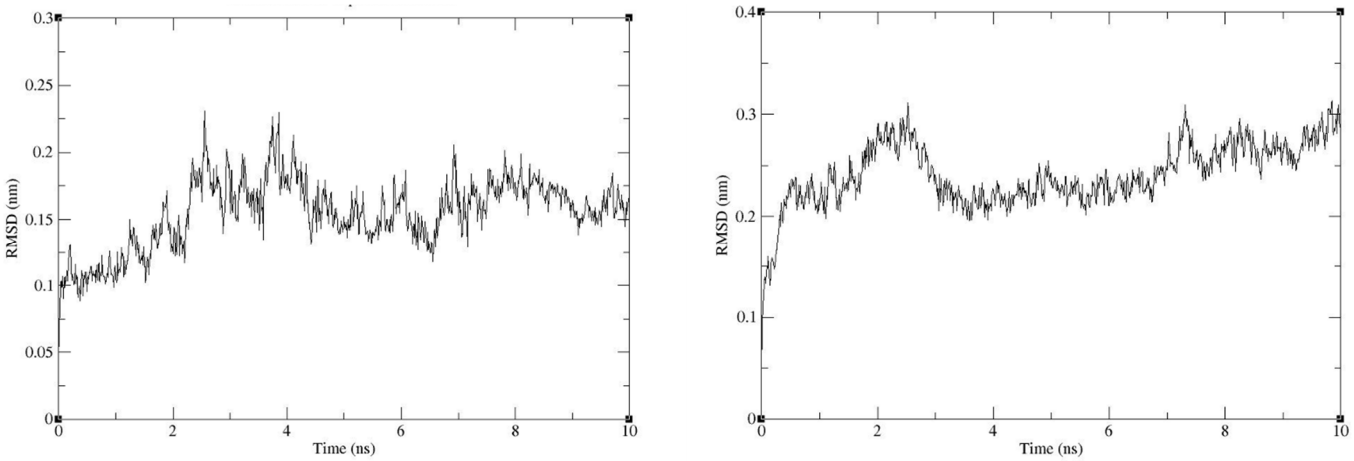

Figure 4. Root mean square deviation (RMSD) values of Hymenidin with SARS-CoV-2 Main Protease during the entire 10 ns in MD.

Preprints (www.preprints.org) | NOT PEER-REVIEWED | Posted: 1 December 2022 doi:10.20944/preprints202212.0008.v1

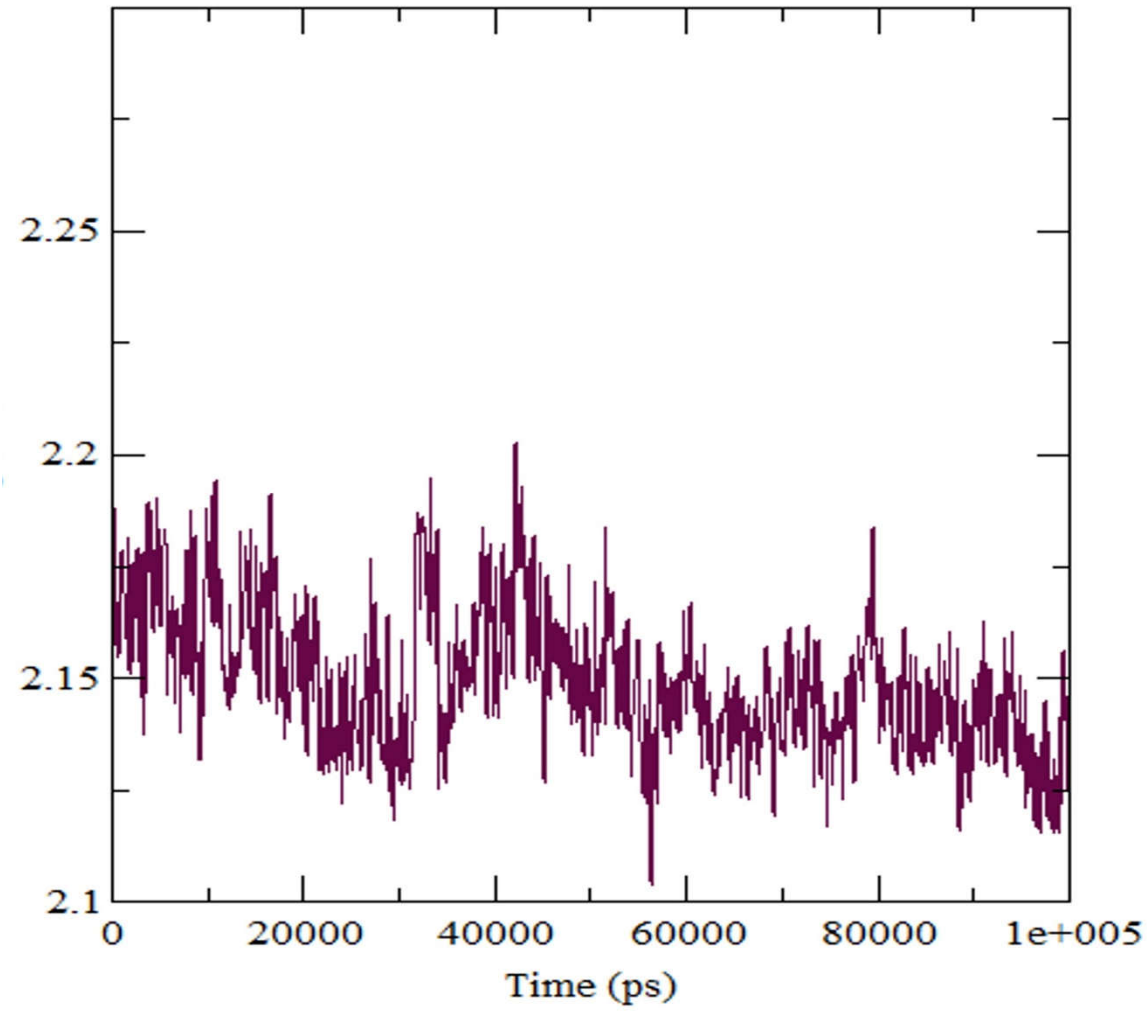

Figure 5. Trajectory of Radius of gyration (ROG) for the SARS-CoV-2 main protease with Hymenidin.

Preprints (www.preprints.org) | NOT PEER-REVIEWED | Posted: 1 December 2022 doi:10.20944/preprints202212.0008.v1

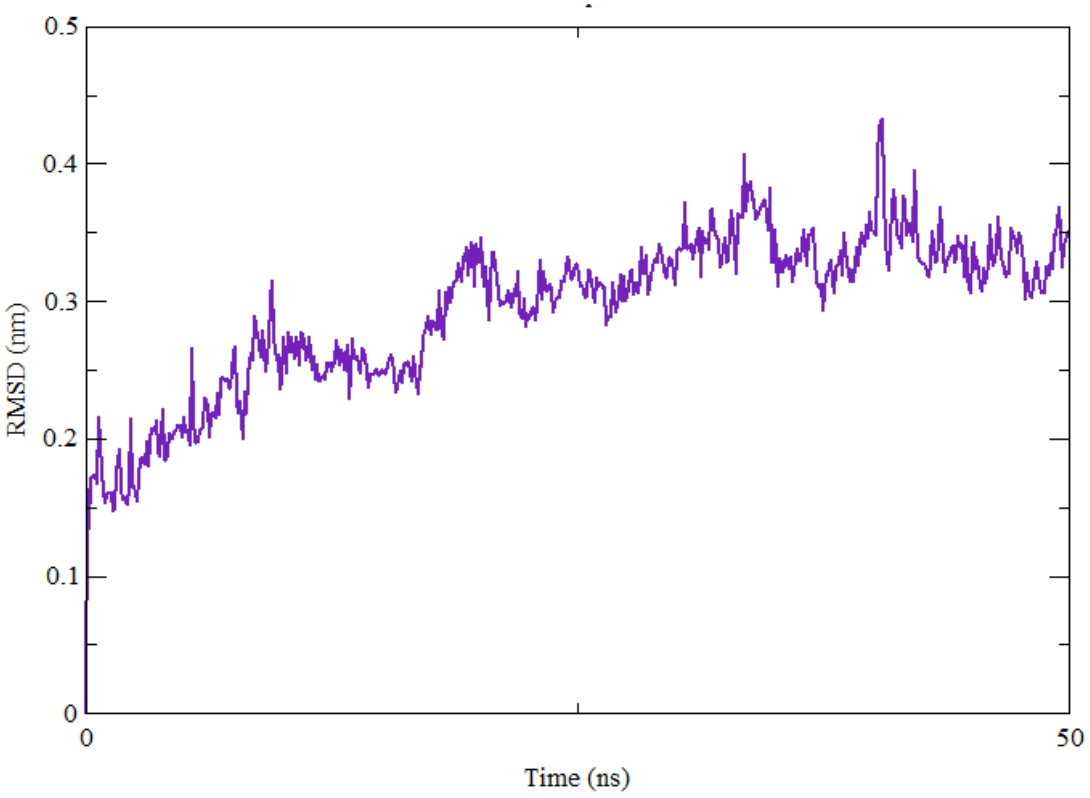

Figure 6. Root mean square deviation (RMSD) values of Hymenidin with SARS-CoV-2 Main Protease during the entire 50 ns in MD.

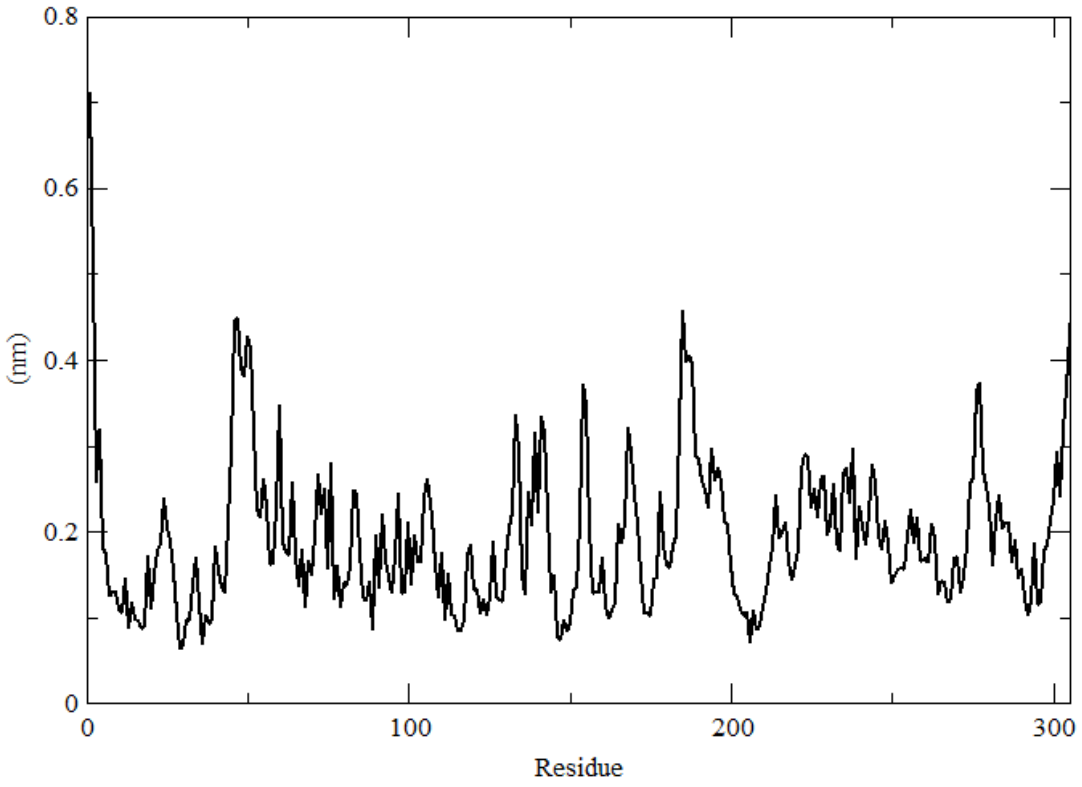

Figure 7. Trajectory of RMSF for the SARS-CoV-2 main protease with Hymenidin.

Preprints (www.preprints.org) | NOT PEER-REVIEWED | Posted: 1 December 2022 doi:10.20944/preprints202212.0008.v1

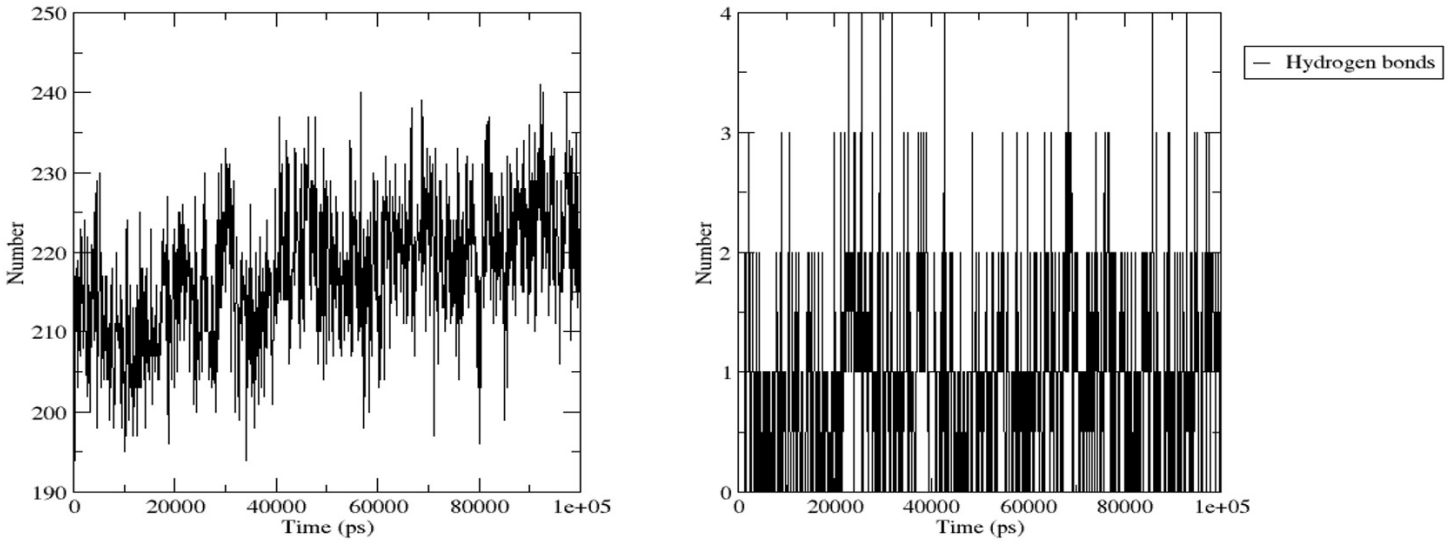

Figure 8. H-bond interaction for the complex between SARS-CoV-2 main protease and Hymenidin.

3.4. Pharmacokinetic properties analysis

In silico ADMET screening has been widely used for drug development and drug discovery process. It is used to minimize the failure rates and reduce the time of drug discovery. Aqueous solubility, intestinal absorption, and membrane permeability are important criteria for the drug development process[43,44]. Aqueous solubility is an important criterion to study the ratio of drug uptake, transfer, and clearance. Gastrointestinal absorption (GIB) and drug distribution are major obstacles in oral drug delivery. The higher intestinal absorption value indicates that the drug has good bioavailability in the system. The five lead MDPs (Chrysophaentin A, Geodisterol sulfates, Hymenidin, Plinabulin (NPI-2358), Tetrodotoxin) against COVID -19 targets were analyzed for ADMET properties using the pkCSM online server. The results of six active compounds with high activity potentials are represented in Table 4. More the 30% of GIB values implies good absorbance. Chrysophaentin A showed the highest percentage of GIB (100%), followed by Hymenidin (71.26%) and Plinabulin (65.66%) which showed good absorption scores. Geodisterol sulfates (49.98%) and Tetrodotoxin (36.93%) displayed a moderate absorption percentage. Skin Permeability (SKP) value greater than − 2.5 cm/h is considered low skin permeability and all five drug candidates were shown acceptable SKP values. Similarly, all five drug candidates displayed low Caco2 permeability (<0.9 cm/s). P-glycoprotein (PGP) is an important drug transporter and it helps to determine the uptake and efflux of a range of drugs. The inhibition of PGP can result in increased bioavailability of the susceptible drug and induction of PGP reduces the bioavailability[45,46]. All five-drug candidates were shown to be a substrate for PGP. Chrysophaentin A and Geodisterol sulfates were both observed to be an inhibitor for PGP.

The VDss, CNS, and BBB membrane permeability were used to study the drug distribution [47]. The greater than log 0.45 value represent the relatively higher distribution volume. All drug candidates exhibited less than log 0.45 value and Plinabulin exhibited the better VDss (0.325) compared to the other four compounds. BBB membrane permeability (range: log BB values > 0.3) and CNS permeability (range of log PS values > − 2 to < − 3) are important parameters in the distribution mechanism. All five marine drug compounds were predicted to be neither capable of crossing the CNS nor BBB membrane. The CYP450 plays a vital role in all drug metabolism and it has two important subtypes: CYP2D6 and CYP3A4. All five compounds were not substrates for the CYP2D6 [48] and similarly, all compounds were not substrates for the CYP3A4 except Chrysophaentin A. Chrysophaentin A, Geodisterol sulfates, Hymenidin, and Tetrodotoxin CYP1A2 inhibitor

 doi:10.20944/preprints202212.0008.v1

were not predicted as a substrate for CYP2C19, CYP2C9, CYP2D6, CYP3A4 inhibitors. Plinabulin was predicted to be an inhibitor for CYP2C19 and CYP3A4. This suggested that Chrysophaentin A and Plinabulin may be metabolized in the liver.

Drug Excretion is related to the MW and hydrophilicity of marine active compounds. There are two important parameters involved in drug excretion i) Total Clearance (TCs) and ii) Renal OCT2 substrate. The TCs is measured by a combination of hepatic and renal clearance[49]. Hymenidin (1.027) showed the highest TCs score followed by Tetrodotoxin (0.663), Plinabulin (0.457), Geodisterol sulfates (0.27), and Chrysophaentin A (-0.211) showed the least TCs score. none of the compounds were predicted as a substrate for Renal OCT2. Toxicity is an important role in the selection of the most suitable drug compounds. AMES toxicity is used to predict the carcinogenic effect of drug compounds[50]. None of the compounds expressed the AMES toxicity except Plinabulin. hERG inhibition (I and II) is an important parameter that is mainly involved in cardiotoxicity[51]. None of the marine drug compounds expressed the inhibitory actions for hERG-I channel. Chrysophaentin A and Plinabulin were involved in the inhibitory actions of hERG-II channel. All compounds were predicted as they may not have skin sensitization and hepatotoxicity (expert Hymenidin). The Maximum tolerated dose (for humans), LD50 and LOAEL values were predicted and tabulated in Table 4.

Preprints (www.preprints.org) | NOT PEER-REVIEWED | Posted: 1 December 2022 doi:10.20944/preprints202212.0008.v1

Table 4. *In silico* ADMET/pharmacokinetic properties analysis of the selected marine derived clinical level compounds using pkCSM web server.

Property	Name	Tetrodotoxin	Chrysophaentin A	Geodisterol sulfates	Hymenidin	Plinabulin	Unit
Absorption	Water solubility	**-2.244**	**-2.898**	**-3.231**	**-2.893**	**-2.894**	log mol/L
	Caco2 permeability	**0.557**	**-0.859**	**0.551**	**-0.336**	**-0.128**	log Papp in 10^{-} cm/s
	Intestinal absorption (human)	**36.93**	**100**	**49.98**	**71.261**	**65.663**	% Absorbed
	Skin Permeability	**-2.735**	**-2.735**	**-2.735**	**-2.735**	**-2.735**	log Kp
	P-glycoprotein substrate	**Yes**	**Yes**	**Yes**	**Yes**	**Yes**	Yes/No
	P-glycoprotein I inhibitor	**No**	**Yes**	**No**	**No**	**No**	Yes/No
	P-glycoprotein II inhibitor	**No**	**Yes**	**Yes**	**No**	**No**	Yes/No
Distribution	VDss (human)	**-1.053**	**-1.24**	**-1.205**	**-0.367**	**0.325**	log L/kg
	Fraction unbound (human)	**0.8**	**0.143**	**0.08**	**0.458**	**0.101**	Numeric (Fu)
	BBB permeability	**-1.149**	**-2**	**-0.893**	**-1.288**	**-0.285**	log BB
	CNS permeability	**-5.174**	**-2.487**	**-2.763**	**-4.592**	**-2.619**	log PS
Metabolism	CYP2D6 substrate	**No**	**No**	**No**	**No**	**No**	Yes/No
	CYP3A4 substrate	**No**	**Yes**	**No**	**No**	**No**	Yes/No
	CYP1A2 inhibitior	**No**	**No**	**No**	**No**	**Yes**	Yes/No
	CYP2C19 inhibitior	**No**	**No**	**No**	**No**	**No**	Yes/No
	CYP2C9 inhibitior	**No**	**No**	**No**	**No**	**No**	Yes/No
	CYP2D6 inhibitior	**No**	**No**	**No**	**No**	**Yes**	Yes/No
	CYP3A4 inhibitior	**No**	**No**	**No**	**No**	**No**	Yes/No
Excretion	Total Clearance score	**0.663**	**-0.211**	**0.27**	**1.027**	**0.457**	log ml/min/kg
	Renal OCT2 substrate	**No**	**No**	**No**	**No**	**No**	Yes/No
Toxicity	AMES toxicity	**No**	**No**	**No**	**No**	**Yes**	Yes/No
	Max. tolerated dose (human)	**0.44**	**0.432**	**-0.098**	**0.551**	**0.424**	log mg/kg/day
	hERG I inhibitor	**No**	**No**	**No**	**No**	**No**	Yes/No
	hERG II inhibitor	**No**	**Yes**	**No**	**No**	**Yes**	Yes/No
	Oral Rat Acute Toxicity (LD50)	**2.061**	**2.512**	**2.686**	**2.507**	**2.669**	mol/kg
	Oral Rat Chronic Toxicity	**5.252**	**2.535**	**2.247**	**2.19**	**1.662**	log mg/kg bw/day
	Hepatotoxicity	**No**	**No**	**No**	**Yes**	**No**	Yes/No
	Skin Sensitisation	**No**	**No**	**No**	**No**	**No**	Yes/No
	T.Pyriformis toxicity	**0.285**	**0.285**	**0.285**	**0.285**	**0.285**	log ug/L
	Minnow toxicity	**7.311**	**-0.711**	**-0.305**	**2.477**	**4.67**	log mM

Abbreviations: VDss: volume of distribution at steady state; BBB: brain blood barrier; CNS: central nervous center; CYP: cytochrome P; OCT: organic cation transporter; hERG: human Ether-a-go-go-Related Gene; LD50: lethal dose of 50 ` %.

4. Conclusion

In summary, 16 marine-derived clinical level compounds were investigated by *in silico* Drug-likeness analysis, molecular docking, and ADMET properties. Among the 16

drug candidates, five compounds proposed the potential hits against the SARS-CoV-2 Main Protease. The present studies have suggested that Chrysophaentin A, Hymenidin, and Tetrodotoxin could be the options to treat COVID-19-associated infections. Due to the encouraging results, further *in vivo* trials are highly recommended for the experimental validation of the present findings.

Author Contributions: Conceptualization, S.M, C.R, A.A,; methodology, V.A and D.K.L; software, P.P, and M.V; validation, ; C.R, A.A; formal analysis, C.K, Z.M; S.U.L; data curation, J.P.L and F.F; writing— original draft preparation, S.M, C.R, M. Y and A.H.M.; writing—review and editing, all authors; visualization, all authors. All authors have read and agreed to the published version of the manuscript.

Funding: This research did not receive any external funds.

Institutional Review Board Statement: Not applicable.

Informed Consent Statement: Not applicable.

Data Availability Statement: All obtained data are presented in this article.

Conflicts of Interest: The authors declare no conflict of interest.

References

1. Abd El-Aziz, T.M.; Stockand, J.D. Recent Progress and Challenges in Drug Development against COVID-19 Coronavirus (SARS-CoV-2)-an Update on the Status. *Infection, Genetics and Evolution* **2020**, *83*, 104327.
2. Idda, M.L.; Soru, D.; Floris, M. Overview of the First 6 Months of Clinical Trials for COVID-19 Pharmacotherapy: The Most Studied Drugs. *Frontiers in public health* **2020**, *8*, 497.
3. Prathiviraj, R.; Saranya, S.; Bharathi, M.; Chellapandi, P. A Hijack Mechanism of Indian SARS-CoV-2 Isolates for Relapsing Contemporary Antiviral Therapeutics. *Computers in biology and medicine* **2021**, *132*, 104315.
4. Prathiviraj, R.; Chellapandi, P.; Begum, A.; Kiran, G.S.; Selvin, J. Identification of Genotypic Variants and Its Proteomic Mutations of Brazilian SARS-CoV-2 Isolates. *Virus research* **2022**, *307*, 198618.
5. Singh, M.; de Wit, E. Antiviral Agents for the Treatment of COVID-19: Progress and Challenges. *Cell Reports Medicine* **2022**, *3*, 100549.
6. Li, H.; Xue, Q.; Xu, X. Involvement of the Nervous System in SARS-CoV-2 Infection. *Neurotoxicity research* **2020**, *38*, 1–7.
7. Varga, Z.; Flammer, A.J.; Steiger, P.; Haberecker, M.; Andermatt, R.; Zinkernagel, A.S.; Mehra, M.R.; Schuepbach, R.A.; Ruschitzka, F.; Moch, H. Endothelial Cell Infection and Endotheliitis in COVID-19. *The Lancet* **2020**, *395*, 1417–1418.
8. Kim, D.; Lee, J.-Y.; Yang, J.-S.; Kim, J.W.; Kim, V.N.; Chang, H. The Architecture of SARS-CoV-2 Transcriptome. *Cell* **2020**, *181*, 914–921.
9. Pal, S.A.R.S. Coronavirus-2 (SARS-CoV-2): An Update.
10. Yoshimoto, F.K. The Proteins of Severe Acute Respiratory Syndrome Coronavirus-2 (SARS CoV-2 or n-COV19), the Cause of COVID-19. *The protein journal* **2020**, *39*, 198–216.
11. Bianchi, M.; Benvenuto, D.; Giovanetti, M.; Angeletti, S.; Ciccozzi, M.; Pascarella, S. Sars-CoV-2 Envelope and Membrane Proteins: Differences from Closely Related Proteins Linked to Cross-Species Transmission. *BioMed Research International* **2020**, *4389089*.
12. Snijder, E.J.; Decroly, E.; Ziebuhr, J. Coronaviruses. **2016**.
13. Jackson, C.B.; Farzan, M.; Chen, B.; Choe, H. Mechanisms of SARS-CoV-2 Entry into Cells. *Nature reviews Molecular cell biology* **2022**, *23*, 3–20.
14. Alanagreh, L.; Alzoughool, F.; Atoum, M. The Human Coronavirus Disease COVID-19: Its Origin, Characteristics, and Insights into Potential Drugs and Its Mechanisms. *Pathogens* **2020**, *9*, 331.
15. Wu, C.; Liu, Y.; Yang, Y.; Zhang, P.; Zhong, W.; Wang, Y.; Wang, Q.; Xu, Y.; Li, M.; Li, X. Analysis of Therapeutic Targets for SARS-CoV-2 and Discovery of Potential Drugs by Computational Methods. *Acta Pharmaceutica Sinica B* **2020**, *10*, 766–788.
16. Salehi, B.; Sharifi-Rad, J.; Seca, A.M.; Pinto, D.C.; Michalak, I.; Trincone, A.; Mishra, A.P.; Nigam, M.; Zam, W.; Martins, N. Current Trends on Seaweeds: Looking at Chemical Composition, Phytopharmacology, and Cosmetic Applications. *Molecules* **2019**, *24*, 4182.
17. Tanna, B.; Mishra, A. Nutraceutical Potential of Seaweed Polysaccharides: Structure, Bioactivity, Safety, and Toxicity. Compr Rev Food Sci Food Saf 18: 817–831 2019.
18. Dyshlovoy, S.A.; Honecker, F. Marine Compounds and Cancer: The First Two Decades of XXI Century. *Marine Drugs* 2019, *18*, 20.
19. Kumar, L.D.; Prathiviraj, R.; Selvakumar, M.; Guna, R.; Abbirami, E.; Sivasudha, T. HRLC-ESI-MS Based Identification of Active Small Molecules from Cissus Quadrangularis and Likelihood of Their Action towards the Primary Targets of Osteoarthritis. *Journal of Molecular Structure* **2020**, *1199*, 127048.

20. Murugesan, S.; Srinivasan, V.; Lakshmanan, D.K.; Venkateswaran, M.R.; Jayabal, S.; Nadar, M.M.; Kathiravan, A.; Jhonsi, M.A.; Thilagar, S.; Periyasamy, S. Evaluation of the Anti-Rheumatic Properties of Thymol Using Carbon Dots as Nanocarriers on FCA Induced Arthritic Rats. *Food & Function* **2021**, *12*, 5038–5050.
21. Lipinski, C.A.; Lombardo, F.; Dominy, B.W.; Feeney, P.J. Experimental and Computational Approaches to Estimate Solubility and Permeability in Drug Discovery and Development Settings. *Advanced drug delivery reviews* **1997**, *23*, 3–25.
22. Pires, D.E.; Blundell, T.L.; Ascher, D.B. PkCSM: Predicting Small-Molecule Pharmacokinetic and Toxicity Properties Using Graph-Based Signatures. *Journal of medicinal chemistry* **2015**, *58*, 4066–4072.
23. Selvakumar, M.; Palanichamy, P.; Arumugam, V.; Venkatesan, M.; Aathmanathan, S.; Krishnamoorthy, H.; Pugazhendhi, A. In Silico Potential of Nutraceutical Plant of Pithecellobium Dulce against GRP78 Target Protein for Breast Cancer. *Applied Nanoscience* **2021**, 1–13.
24. Abraham, M.J.; Murtola, T.; Schulz, R.; Páll, S.; Smith, J.C.; Hess, B.; Lindahl, E. GROMACS: High Performance Molecular Simulations through Multi-Level Parallelism from Laptops to Supercomputers. *SoftwareX* **2015**, *1*, 19–25.
25. Tian, C.; Kasavajhala, K.; Belfon, K.A.; Raguette, L.; Huang, H.; Migues, A.N.; Bickel, J.; Wang, Y.; Pincay, J.; Wu, Q. Ff19SB: Amino-Acid-Specific Protein Backbone Parameters Trained against Quantum Mechanics Energy Surfaces in Solution. *Journal of chemical theory and computation* **2019**, *16*, 528–552.
26. Sousa da Silva, A.W.; Vranken, W.F. ACPYPE-Antechamber Python Parser Interface. *BMC research notes* **2012**, *5*, 1–8.
27. Wang, W.R.; Wolf, R. J.; Caldwell, JW; Kollman, PA; Case. *DA Journal of Computational Chemistry* **2004**, *25*, 92.
28. Wang, J.; Wang, W.; Kollman, P.A.; Case, D.A. Automatic Atom Type and Bond Type Perception in Molecular Mechanical Calculations. *Journal of molecular graphics and modelling* **2006**, *25*, 247–260.
29. Salgarello, M.; Visconti, G.; Barone-Adesi, L. Interlocking Circumareolar Suture with Undyed Polyamide Thread: A Personal Experience. *Aesthetic plastic surgery* **2013**, *37*, 1061–1062.
30. Hammad, S.; Bouaziz-Terrachet, S.; Meghnem, R.; Meziane, D. Pharmacophore Development, Drug-Likeness Analysis, Molecular Docking, and Molecular Dynamics Simulations for Identification of New CK2 Inhibitors. *Journal of Molecular Modeling* **2020**, *26*, 1–17.
31. Yusof, I.; Segall, M.D. Considering the Impact Drug-like Properties Have on the Chance of Success. *Drug Discovery Today* **2013**, *18*, 659–666.
32. Hu, Q.; Xiong, Y.; Zhu, G.-H.; Zhang, Y.-N.; Zhang, Y.-W.; Huang, P.; Ge, G.-B. The SARS-CoV-2 Main Protease (Mpro): Structure, Function, and Emerging Therapies for COVID-19. *MedComm* **2022**, *3*, e151.
33. Vishvakarma, V.K.; Singh, M.B.; Jain, P.; Kumari, K.; Singh, P. Hunting the Main Protease of SARS-CoV-2 by Plitidepsin: Molecular Docking and Temperature-Dependent Molecular Dynamics Simulations. *Amino acids* **2022**, *54*, 205–213.
34. Rauf, A.; Rashid, U.; Khalil, A.A.; Khan, S.A.; Anwar, S.; Alafnan, A.; Alamri, A.; Rengasamy, K.R. Docking-Based Virtual Screening and Identification of Potential COVID-19 Main Protease Inhibitors from Brown Algae. *South African Journal of Botany* **2021**, *143*, 428–434.
35. Ghosh, S.; Das, S.; Ahmad, I.; Patel, H. In Silico Validation of Anti-Viral Drugs Obtained from Marine Sources as a Potential Target against SARS-CoV-2 Mpro. *Journal of the Indian Chemical Society* **2021**, *98*, 100272.
36. Ramadhan, D.S.F.; Siharis, F.; Abdurrahman, S.; Isrul, M.; Fakih, T.M. In Silico Analysis of Marine Natural Product from Sponge (Clathria Sp.) for Their Activity as Inhibitor of SARS-CoV-2 Main Protease. *Journal of Biomolecular Structure and Dynamics* **2021**, 1–7.
37. Swain, S.S.; Singh, S.R.; Sahoo, A.; Panda, P.K.; Hussain, T.; Pati, S. Integrated Bioinformatics–Cheminformatics Approach toward Locating Pseudo-Potential Antiviral Marine Alkaloids against SARS-CoV-2-Mpro. *Proteins: Structure, Function, and Bioinformatics* **2022**.
38. Baildya, N.; Ghosh, N.N.; Chattopadhyay, A.P. Inhibitory Activity of Hydroxychloroquine on COVID-19 Main Protease: An Insight from MD-Simulation Studies. *Journal of Molecular Structure* **2020**, *1219*, 128595.
39. Teli, D.M.; Shah, M.B.; Chhabria, M.T. In Silico Screening of Natural Compounds as Potential Inhibitors of SARS-CoV-2 Main Protease and Spike RBD: Targets for COVID-19. *Frontiers in molecular biosciences* **2021**, *7*, 599079.
40. Krupanidhi, S.; Abraham Peele, K.; Venkateswarulu, T.C.; Ayyagari, V.S.; Nazneen Bobby, M.; John Babu, D.; Venkata Narayana, A.; Aishwarya, G. Screening of Phytochemical Compounds of Tinospora Cordifolia for Their Inhibitory Activity on SARS-CoV-2: An in Silico Study. *Journal of Biomolecular Structure and Dynamics* **2021**, *39*, 5799–5803.
41. Singh, M.B.; Vishvakarma, V.K.; Lal, A.A.; Chandra, R.; Jain, P.; Singh, P. A Comparative Study of 5-Fluorouracil, Doxorubicin, Methotrexate, Paclitaxel for Their Inhibition Ability for Mpro of NCoV: Molecular Docking and Molecular Dynamics Simulations. *Journal of the Indian Chemical Society* **2022**, 100790.
42. Chen, D.; Oezguen, N.; Urvil, P.; Ferguson, C.; Dann, S.M.; Savidge, T.C. Regulation of Protein-Ligand Binding Affinity by Hydrogen Bond Pairing. *Science advances* **2016**, *2*, e1501240.
43. Aungst, B.J. Optimizing Oral Bioavailability in Drug Discovery: An Overview of Design and Testing Strategies and Formulation Options. *Journal of pharmaceutical sciences* **2017**, *106*, 921–929.
44. Bergström, C.A. In Silico Predictions of Drug Solubility and Permeability: Two Rate-Limiting Barriers to Oral Drug Absorption. *Basic & clinical pharmacology & toxicology* **2005**, *96*, 156–161.
45. Igel, S.; Drescher, S.; Mürdter, T.; Hofmann, U.; Heinkele, G.; Tegude, H.; Glaeser, H.; Brenner, S.S.; Somogyi, A.A.; Omari, T. Increased Absorption of Digoxin from the Human Jejunum Due to Inhibition of Intestinal Transporter-Mediated Efflux. *Clinical pharmacokinetics* **2007**, *46*, 777–785.

 doi:10.20944/preprints202212.0008.v1

46. König, J.; Müller, F.; Fromm, M.F. Transporters and Drug-Drug Interactions: Important Determinants of Drug Disposition and Effects. *Pharmacological reviews* **2013**, *65*, 944–966.
47. Han, Y.; Zhang, J.; Hu, C.Q.; Zhang, X.; Ma, B.; Zhang, P. In Silico ADME and Toxicity Prediction of Ceftazidime and Its Impurities. *Frontiers in pharmacology* **2019**, *10*, 434.
48. Bibi, Z. Role of Cytochrome P450 in Drug Interactions. *Nutrition & metabolism* **2008**, *5*, 1–10.
49. Shargel, L.; Wu-Pong, S.; Yu, A.B.C. Chapter 6. Drug Elimination and Clearance. *Applied Biopharmaceutics & Pharmacokinetics. 6th Edition. New York (NY): The McGraw-Hill Companies* **2012**, 106.
50. Kirkland, D.; Zeiger, E.; Madia, F.; Gooderham, N.; Kasper, P.; Lynch, A.; Morita, T.; Ouedraogo, G.; Morte, J.M.P.; Pfuhler, S. Can in Vitro Mammalian Cell Genotoxicity Test Results Be Used to Complement Positive Results in the Ames Test and Help Predict Carcinogenic or in Vivo Genotoxic Activity? I. Reports of Individual Databases Presented at an eurl ecvam Workshop. *Mutation Research/Genetic Toxicology and Environmental Mutagenesis* **2014**, *775*, 55–68.
51. Creanza, T.M.; Delre, P.; Ancona, N.; Lentini, G.; Saviano, M.; Mangiatordi, G.F. Structure-Based Prediction of HERG-Related Cardiotoxicity: A Benchmark Study. *Journal of Chemical Information and Modeling* **2021**, *61*, 4758–4770.